Organic Geochemistry 194 (2024) 104815

Contents lists available at ScienceDirect

Organic Geochemistry

journal homepage: www.elsevier.com/locate/orggeochem

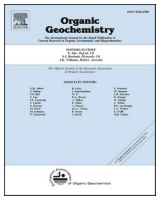

New practical biodegradation proxies based on heteroatom compounds revealed by ESI (−) FT-ICR MS

Shuo Deng [a,b], Sumei Li [a,b,*], Xiaoyan Li [c]

[a] State Key Laboratory of Petroleum Resources and Engineering, China University of Petroleum (Beijing), Beijing 102249, China
[b] College of Geoscience, China University of Petroleum (Beijing), Beijing 102249, China
[c] Research Institute of Petroleum Exploration & Development, PetroChina Huabei Oilfield Company, Renqiu, Hebei 062552, China

ARTICLE INFO

Associate Editor - Guangyou Zhu

Keywords:
ESI FT-ICR MS
Heavy oil
Biodegradation
Heteroatomic compound
Liaohe Western Depression

ABSTRACT

High-resolution mass spectrometry can be utilized to select specific proxies for the quantitative assessment of crude oil biodegradation degree, offering higher accuracy and convenience compared to conventional GC-MS methods. However, the current evaluation proxies are invalid for severely biodegraded crude oil. In this study, freshwater and saltwater lacustrine crude oils from the Liaohe Western Depression (Bohai Bay Basin) with varying degrees of degradation, were characterized using negative ion electrospray ionization [ESI (−)] Fourier transform ion cyclotron resonance mass spectrometry (FT-ICR MS). The results show that seven heteroatom classes were identified including N_1, N_1O_1, N_1O_2, O_1, O_2, O_3 and O_4. Certain differences exist in the abundance of heteroatom compounds in the nondegraded crude oils from the two origins, but both are dominated by N_1. The relative abundance of O_2 class species significantly increases, while the relative abundance of O_1 and N_1 class species decreases with an increase in the degree of biodegradation, reflecting the increase in the content of acid compounds as biodegradation products. O_2 class species become the predominant compound in the severe degradation stage. Biodegradation results in the enrichment of compounds with greater condensation, while the abundance of highly alkyl-substituted compounds decreases. The nitrogen-containing compound pairing proxies ($DBE_{12,13,15}/DBE_{9\sim11}$-$N_1$) can be employed to assess the degree of biodegradation in crude oil under conditions of similar maturity. As the degree of biodegradation increases, the content of 2 ~ 5-cyclic naphthenic acids increase, while the content of acyclic acids with weaker resistance to degradation decreases. The ratio of acyclic acids to 2 ~ 5-cyclic naphthenic acids (Modified A/C Ratio 2) can effectively assess the biodegradation level of crude oils ranging from nondegraded to severe degradation. The $O_2/(N_1 + O_1)$ Ratio reflects the formation of acids during the biodegradation process and exhibits a robust positive correlation with crude oil density and degradation degree. The new proxies provide higher precision and broader applicability compared to conventional methods, enabling quantitative evaluation of biodegradation levels. The application of ESI FT-ICR MS technology holds significant importance in the assessment of heavy oil and the exploration of its genetic mechanisms.

1. Introduction

Heavy oil represents a substantial petroleum resource, with global reserves approximately three times that of the combined total volume of conventional crude oil and natural gas (Hein, 2017; Liu et al., 2019). Biodegradation stands out as a prevalent secondary alteration process within oil reservoirs, and the formation of most heavy oils worldwide is intricately linked to this phenomenon (Larter et al., 2006). Crude oil typically contains fewer heteroatom compounds, typically containing oxygen, sulfur, and/or nitrogen atoms, but their concentrations are higher in heavy oil compared to conventional crude oil. As the process of biodegradation intensifies, lower molecular weight hydrocarbons undergo degradation, giving rise to heteroatomic compounds (Connan, 1984; Kim et al., 2005; Larter et al., 2006), which results in an increase in the polarity, density, viscosity and acidity of the crude oil (Connan, 1984). For severely biodegraded crude oil samples rich in polar components, the hydrocarbon fraction is heavily altered, generally resulting in the presence of unresolved complex mixtures (UCM), which are difficult to identify using GC-MS (Meredith et al., 2000). Traditional GC-MS techniques are employed to qualitatively evaluate the degree of

* Corresponding author.
E-mail address: smli@cup.edu.cn (S. Li).

https://doi.org/10.1016/j.orggeochem.2024.104815
Received 27 December 2023; Received in revised form 4 June 2024; Accepted 4 June 2024
Available online 12 June 2024

biodegradation in crude oil by identifying the presence or absence of specific compounds (Peters et al., 2005; Wenger et al., 2002). Nevertheless, the currently prevalent scales employed to characterize the extent of petroleum biodegradation lack the necessary resolution to effectively assess many heavily biodegraded heavy oils and bitumen (Adams et al., 2008; Larter et al., 2012).

In recent years, the combination of electrospray ionization (ESI) and Fourier transform ion cyclotron resonance mass spectrometry (FT-ICR MS), which has been widely applied in the field of biomolecular analysis, has successfully solved the traditional problem of polar compound analysis in petroleum molecules (Qian et al., 2001a; Zhan and Fenn, 2000). Currently, several application results have been achieved, including reconstructing sedimentary paleoenvironments (Ji et al., 2018; Rocha et al., 2018; Wan et al., 2017), evaluating the maturity of crude oils or source rocks (Hughey et al., 2004; Ji et al., 2018; Wan et al., 2017), revealing petroleum migration pathways (Liu et al., 2015; Zhang et al., 2016; Ziegs et al., 2018), and deciphering the genesis of high acid value crude oil (Li et al., 2010a) and biodegraded heavy oil (Hughey et al., 2007; Hughey et al., 2008; Kim et al., 2005; Liao et al., 2012; Liu et al., 2020; Pan et al., 2017; Pan et al., 2013). Several previous studies

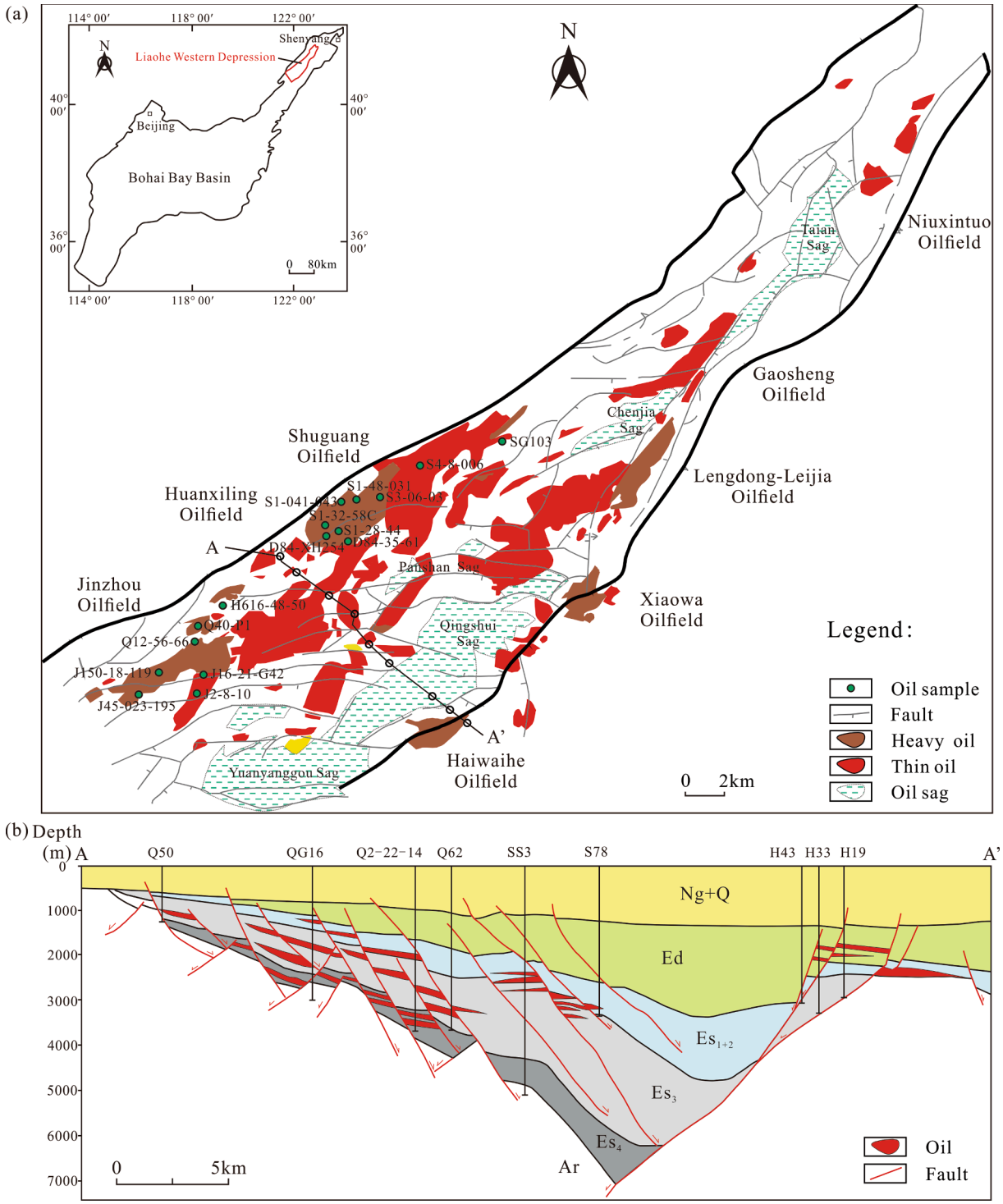

Fig. 1. (a) Regional structural map depicting the location of the Liaohe Western Depression; (b) cross-sectional view of the Liaohe Western Depression.

have employed ESI FT-ICR MS to investigate the impacts of mild to moderate biodegradation on NSO compounds in crude oils, conducted under both natural and laboratory conditions (Hughey et al., 2007; Kim et al., 2005; Liu et al., 2020; Pan et al., 2017; Pan et al., 2013). Furthermore, heteroatom compound proxies, such as the ratio of acyclic acids to 1 ~ 3-cyclic naphthenic acids (A/C Ratio), have been proposed as alternative for evaluating biodegradation (Kim et al., 2005; Martins et al., 2017; Vaz et al., 2013). ESI FT-ICR MS technology enables the quantitative assessment of crude oil degradation levels using one or two characteristic proxies, offering the advantages of rapid analysis and high-resolution accuracy. Nonetheless, the presently proposed characteristic proxies are unsuitable for severely biodegraded crude oils (Angolini et al., 2015; Hughey et al., 2007), and a systematic quantitative evaluation index for the degree of biodegradation has yet to be established.

The Liaohe Western Depression in the Bohai Bay Basin is abundant in oil and gas resources, where heavy oil constitutes approximately 46.3 % of the total reserves (Chen et al., 2023). Biodegradation serves as the primary cause of heavy oil formation (Li et al., 2008). Previous studies on Liaohe heavy oil have predominantly emphasized conventional geochemical methods (Huang et al., 2003, 2004; Li et al., 2008), with insufficient investigation into heteroatom compounds (Liao et al., 2012). In this study, freshwater lacustrine and saltwater lacustrine oils with naturally occurring biodegradable sequences (from nondegraded to severely biodegraded) are obtained from the Liaohe Western Depression for ESI (−) FT-ICR MS analysis. The study investigates the impact of biodegradation on the distribution of nitrogen and oxygen compounds in crude oil and their genetic mechanism with an aim to establish a high-resolution scale to evaluate the extent of biodegradation in slightly to severely biodegraded crude oils, introducing a novel approach for the application of heteroatomic compounds.

2. Geological setting

The Liaohe Western Depression is a significant oil-bearing depression in the Bohai Bay Basin, well-known for its abundant heavy oil resources. It spans an area of approximately 2560 km^2 and represents a mid-to-late Cenozoic rift basin with a distribution of northeastward trend. It exhibits features of broken in the east and overlapped in the west, with the eastern side being steep and the western side being gentle (Qi et al., 2013) (Fig. 1a). The Cenozoic structural evolution of the Western Depression is divided into five main stages: the initial rifting period (Es_4), deep rifting period (Es_3), rerifting period (Es_{1+2}), decay regression period (Ed) and depression period (Ng ~ Q) (Qi et al., 2013). The sedimentary strata in the study area can be divided from bottom to top into the Archean/Paleozoic/Mesozoic basement, the Paleogene Fangshenpao Formation, Shahejie Formation (Es), Dongying Formation (Ed), Neogene Guantao Formation (Ng), Minghuazhen Formation (Nm), and the Quaternary deposits (Q). The Es is subdivided into four members (Es_1 to Es_4) (Fig. 1b). The study area predominantly comprises two sets of source rocks: Es_3 and Es_4 (Li et al., 2008; Wang et al., 2011). The Es_3 source rocks were formed in a freshwater lacustrine environment, with Type II kerogen being the dominant type. Conversely, the Es_4 source rocks were formed in a strongly reducing saltwater lacustrine environment, characterized by the predominant Type I kerogen (Li et al., 2008; Wang et al., 2011).

The Liaohe Western Depression host the distribution of heavy oil mainly in the Shuguang, Jinzhou-Huanxiling, Lengdong-Leijia, Gaosheng, Xiaowa and Haiwaihe oilfields (Fig. 1a), primarily in the Es and its upper strata. It exhibits characteristics such as surrounding the oil-generating sag, being located in structurally elevated areas and having shallow burial depths (Li et al., 2008). The oils from Jinzhou-Huanxiling oilfield are moderately mature and primarily sourced from the freshwater Es_3 source rocks. The oils from Shuguang oilfield have lower maturity and are mainly sourced from the saltwater Es_4 source rocks (Li et al., 2008; Xiong et al., 2003).

3. Sample and methods

This study collected 16 crude oils from different biodegradation levels in the Liaohe Western Depression. Among them, seven oils from the Jinzhou-Huanxiling oilfield (JZ) and nine oils from the Shuguang oilfield (SG) (Fig. 1a). All samples were subjected to analysis using GC–MS for saturated hydrocarbons and aromatic hydrocarbons, as well as whole oil analysis using ESI (−) FT-ICR MS.

3.1. GC-MS

An Agilent 6890, equipped with a HP-5MS fused silica capillary column (25 m length, 0.25 mm inner diameter), coupled with an Agilent 5975 mass spectrometric selective detector was employed for GC/MS analysis of the analysis of saturated and aromatic hydrocarbon fractions. Helium was used as the carrier gas, and the temperature program involved a heating rate of 4 °C/min from 100 °C to 220 °C, followed by a further increase to 300 °C at a rate of 2 °C/min. The mass spectrometry ionization energy was set at 70 V. The detailed experimental procedures were described elsewhere (Li et al., 2010b).

3.2. ESI (−) FT-ICR MS

The ESI (−) FT-ICR MS was employed for the analysis of neutral nitrogen and oxygen compounds. To prepare the sample, 10 mg of crude oil/chloroform extract was dissolved in 1 mL of xylene, resulting in a solution with a concentration of 10 mg/mL. A volume of 25 μL was taken, mixed with a xylene-methanol solution (volume ratio of 1:1) and diluted to 1 mL. Subsequently, 15 μL of 28 % ammonium hydroxide was added, and the solution was gently shaken to ensure uniform mixing. Except for the 10 μL Hamilton syringe with a stainless-steel plunger, all other instrument parts used glassware to handle the solvent. Analysis was conducted using a Bruker Apex ultra FT-ICR mass spectrometer equipped with a superconducting 9.4 T magnet. The solution was introduced into the instrument via an injection pump through the Apollo II ion source at a sample flow rate of 150 μL/h. Negative ion formation conditions included a polarization voltage of 4.0 kV, and the capillary entrance and exit voltages were set at 4.5 kV and −320 V, respectively. The ions were stored for 0.1 s in the hexapole ion source. All ions were then accumulated in the hexapole collision cell filled with argon, with an ion storage time of 1 s. Electrostatic focusing was employed to transfer ions into the ICR, with a transition time of 1.2 ms. The ICR mass spectrometry operating conditions included an excitation attenuation of 10 dB, a mass range of 200 ~ 1000 Da, a data size of 2 M, and a time-domain signal accumulation of 256 times. Data processing procedures were described elsewhere (Shi et al., 2010b).

4. Geochemical characteristics of the crude oils

4.1. Physical properties and group compositions

The analyzed crude oil samples encompass both conventional and heavy oil. The JZ crude oils exhibit a density ranging from 0.80 g/cm^3 to 0.99 g/cm^3 and a viscosity ranging from 2.47 mPa·s to 16221.80 mPa·s (Table 1). A general gradual increase in both viscosity and density can be observed as the depth decreases. The SG crude oils display a density range of 0.82 g/cm^3 to 0.99 g/cm^3, accompanied by a viscosity range of 3.73 mPa·s to 46360.91 mPa·s. The crude oils exhibit a saturated hydrocarbon content ranging from 24.62 % to 72.60 % and an aromatic hydrocarbon content ranging from 14.10 % to 41.10 %. The non-hydrocarbon and asphaltene content varies from 11.60 % to 53.41 %. The group composition characteristics of the crude oils are consistent with the physical properties of the crude oil.

Table 1
Basic geochemical parameters of oil from the Liaohe Western Depression (The samples are grouped by the oil field and in the order of the PM biodegradation level).

Oil field	Well	Strata	Depth(m)	PM	Density (g/cm^3)	Viscosity(mPa·s)	Sat(%)	Aro(%)	Non+Asp(%)	Pr/Ph	Pr/nC_{17}	Ph/nC_{18}	G/C_{30}H	C_{35}/C_{34}H	C_{19}/C_{23}TT	C_{29}/C_{30}H	C_{29} 20S	C_{29} αββ	Ts/(Ts + Tm)	C_{29}Ts/C_{30}H	DBT/P
JZ	J2-8-10	Es_3	2483.90	0	0.80	2.47	72.60	15.00	12.40	1.42	0.39	0.28	0.04	0.60	0.41	0.36	0.52	0.40	0.62	0.18	0.09
JZ	J150-18-119	Mz	–	0	0.81	6.10	68.70	14.10	17.20	1.00	0.19	0.20	0.12	0.58	0.31	0.42	0.49	0.53	0.70	0.23	0.16
JZ	Q40-P1	Es_3	982.95	4	0.97	2639.00	56.60	31.10	12.30	–	–	–	0.05	0.64	0.40	0.31	0.50	0.42	0.69	0.18	0.09
JZ	J45-023-195	Es_2	1101.50	6	0.96	2207.90	43.40	29.10	27.50	–	–	–	–	–	–	–	–	–	–	–	–
JZ	J16-21-G42	Es_1	1130.75	6	0.98	16221.80	35.00	31.80	33.20	–	–	–	–	–	–	–	–	–	–	–	–
JZ	H616-48-50	Es_3	920.60	6	0.98	8791.32	38.60	27.30	34.10	–	–	–	–	–	–	–	–	–	–	–	–
JZ	Q12-56-66	Es_2	761.70	7	0.99	3821.00	43.00	30.70	26.20	–	–	–	–	–	–	–	–	–	–	–	–
SG	SG103	Buried hill	1786.80	0	0.82	3.73	72.70	15.70	11.60	0.56	0.31	0.63	0.40	0.56	0.16	0.33	0.39	0.35	0.27	0.05	0.06
SG	S4-8-006	Es_4	1199.50	2	0.91	258.07	40.60	23.40	35.90	0.47	1.46	4.48	0.33	0.66	0.14	0.27	0.35	0.28	0.25	0.04	0.06
SG	S3-06-03	Es_4	1307.35	2	0.88	120.00	51.70	25.20	23.10	0.53	1.12	2.92	0.33	0.68	0.12	0.29	0.36	0.30	0.28	0.04	0.06
SG	S1-32-58C	Es_4	1093.05	3	0.93	1539.30	38.20	30.50	31.40	0.45	1.53	4.52	0.32	0.65	0.16	0.26	0.32	0.27	0.26	0.04	0.09
SG	S1-28-44	Es_4	1481.70	3	0.92	565.74	34.50	33.30	32.20	0.45	3.19	8.80	0.34	0.70	0.17	0.25	0.30	0.28	0.27	0.04	0.09
SG	S1-48-031	Ed	995.90	4	0.95	8671.89	29.80	41.10	29.10	–	–	–	0.33	0.64	0.14	0.26	0.37	0.35	0.25	0.04	0.17
SG	S1-041-043	Buried hill	1126.50	4	0.96	46360.91	28.50	30.50	41.00	–	–	–	0.53	0.65	0.22	0.31	0.36	0.30	0.27	0.05	0.18
SG	D84-35-61	Es_{1-2}	773.35	5	0.97	15326.10	24.62	21.97	53.41	–	–	–	–	–	–	–	–	–	–	–	–
SG	D84-XH254	Es_2	1066.65	7	0.99	6369.22	28.80	29.20	42.10	–	–	–	–	–	–	–	–	–	–	–	–

Note: PM: PM scale; Pr/Ph: pristane/phytane; Pr/nC_{17}: pristane/nC_{17}; Ph/nC_{18}: phytane/nC_{18}; G/C_{30}H: gammacerane/C_{30} hopane; C_{35}/C_{34}H: C_{35}/C_{34} hopane; C_{19}/C_{23}TT: C_{19}/C_{23} tricyclic terpane; C_{29}/C_{30}H: C_{29}/C_{30} hopane; C_{29}20S: C_{29} sterane ααα20S/(20S + 20R); C_{29}αββ: C_{29} steranes αββ/(ααα + αββ); Ts/(Ts + Tm) = 18α(H)-/(18α(H) + 17α(H))-trisnorhopane ratio; C_{29}Ts/C_{30}H: C_{29}Ts/C_{30} hopane; DBT/P: Dibenzothiophene/Phenanthrene.

4.2. Conventional geochemical characteristics

Total ion chromatograms (TIC) of saturated hydrocarbons of all 16 samples are presented in Fig. 2a. Based on the PM scale classification scheme of Peters et al. (2005), J2-8-10, J150-18-119 and SG103 exhibit a complete preservation of normal alkanes (Fig. 2a), indicating that they are not biodegraded (PM = 0). The normal alkanes of S4-8-006, S3-06-03, S1-32-58C and S1-28-44 were partly degraded, and the isoprenoid alkanes were slightly degraded (Fig. 2a), indicating the PM = 1 ~ 3.

The *n*-alkanes of Q40-P1, S1-48-031 and S1-041-043 were not detected, and the isoprenoid alkanes became traces or complete depletion (Fig. 2a), indicating PM = 4. The isoprenoid alkanes of D84-35-61 were entirely depleted (Fig. 2a), but there was no presence of C_{25} norhopanes (Fig. 3b), indicating PM = 5. The hopanes and steranes of J45-023-195, J16-21-G42, H616-48-50, Q12-56-66 and D84-XH254 were obviously altered (Fig. 2a and 3a), and the *m/z* 177 mass chromatogrom shows the presence of C_{25}-norhopanes with carbon numbers ranging from 28 to 29 in J45-023-195, J16-21-G42, H616-48-50, Q12-56-66 and D84-XH254 (Fig. 3b), indicating severe biodegradation (PM = 6 ~ 7).

The Pr/Ph values of nondegraded to moderately biodegraded JZ and SG crude oils were 1.00 ~ 1.42 (average 1.21) and 0.45 ~ 0.56 (average 0.49), respectively. These values suggest that the source rocks for the two groups of oils were formed in weakly oxidizing-weakly reducing and strongly reducing sedimentary environments, respectively (Fig. S1a) (Connan and Cassou, 1980). The cross plot of pristane/phytane (Pr/Ph) versus dibenzothiophene/phenanthrene (DBT/P) can be used to identify palaeosedimentary environment (Hughes et al., 1995). The JZ oils aggregated in Zone D, indicating a lacustrine environment, while the SG oils clusters in Zone C, representing a typical saline lacustrine environment (Fig. S1b).

The *m/z* 191 mass chromatograms of the JZ oils show a relatively low content of gammacerane, with gammacerane/C_{30} hopane ratios ranging from 0.04 to 0.12 (average 0.07) (Fig. S1c), indicating that the source rocks were formed in freshwater environment and/or in depositional setting with less pronounced water column stratification (Peters et al., 2005). The lower C_{35}/C_{34} hopane ratios (0.58 ~ 0.64, average 0.61) are consistent with the typical characteristics of freshwater lacustrine oil (Fig. S1c) (Peters et al., 2005). The gamacerane/C_{30} hopane ratios of SG oils range from 0.32 to 0.53 (average 0.37), and the C_{35}/C_{34} hopane ratios range from 0.56 to 0.70 (average 0.65) (Fig. S1c). These values are higher than those of the JZ oils, indicating that the source rocks were formed in a saline reducing depositional environment (Peters et al., 2005). The higher C_{19}/C_{23} tricyclic terpane and C_{29}/C_{30} hopane ratios generally signify the input of terrestrial organic matter (Peters et al., 2005), indicating a significant contribution of terrestrial material in the JZ oils (Fig. S1d).

The *m/z* 217 mass chromatogram shows that the fingerprints of C_{27}-C_{28}-C_{29} regular steranes in JZ oils generally appears as a "V" shape. while in SG oils, they exhibit a reverse "L" shape (Fig. 2b). This indicates significant differences in their genetic types, with the latter showing agreater input of phytoplankton green algae (Derenne et al., 1992; Grantham, 1986; Volkman, 1986). The C_{29} sterane ααα20S/(20S + 20R) and C_{29} sterane αββ/(αββ + ααα) ratios of JZ oils are 0.49 ~ 0.52 (average 0.50) and 0.40 ~ 0.53 (average 0.45), respectively (Fig. S1e), indicating that the JZ oils are mature (Difan et al., 1990). In contrast, the C_{29} sterane ααα20S/(20S + 20R) (0.30 ~ 0.39, average 0.35) and C_{29} sterane αββ/(αββ + ααα) (0.27 ~ 0.35, average 0.31) ratios of SG oils are relativley low (Fig. S1e), suggesting that the SG oils are at a lower-maturity stage (Difan et al., 1990). The maturity parameters Ts/(Ts + Tm) and C_{29}Ts/C_{30} hopane similarly indicate that JZ crude oil is mature oil while SG crude oil is marginally mature (Fig. S1f) (Peters et al., 2005). In summary, the source rocks of JZ oils were deposited in a weakly oxidizing-weakly reducing freshwater environment, with a mixed origin of type II and III kerogens (Fig. S1a, b). It represents a mature oil with similar maturity levels (Fig. S1e). On the other hand, the

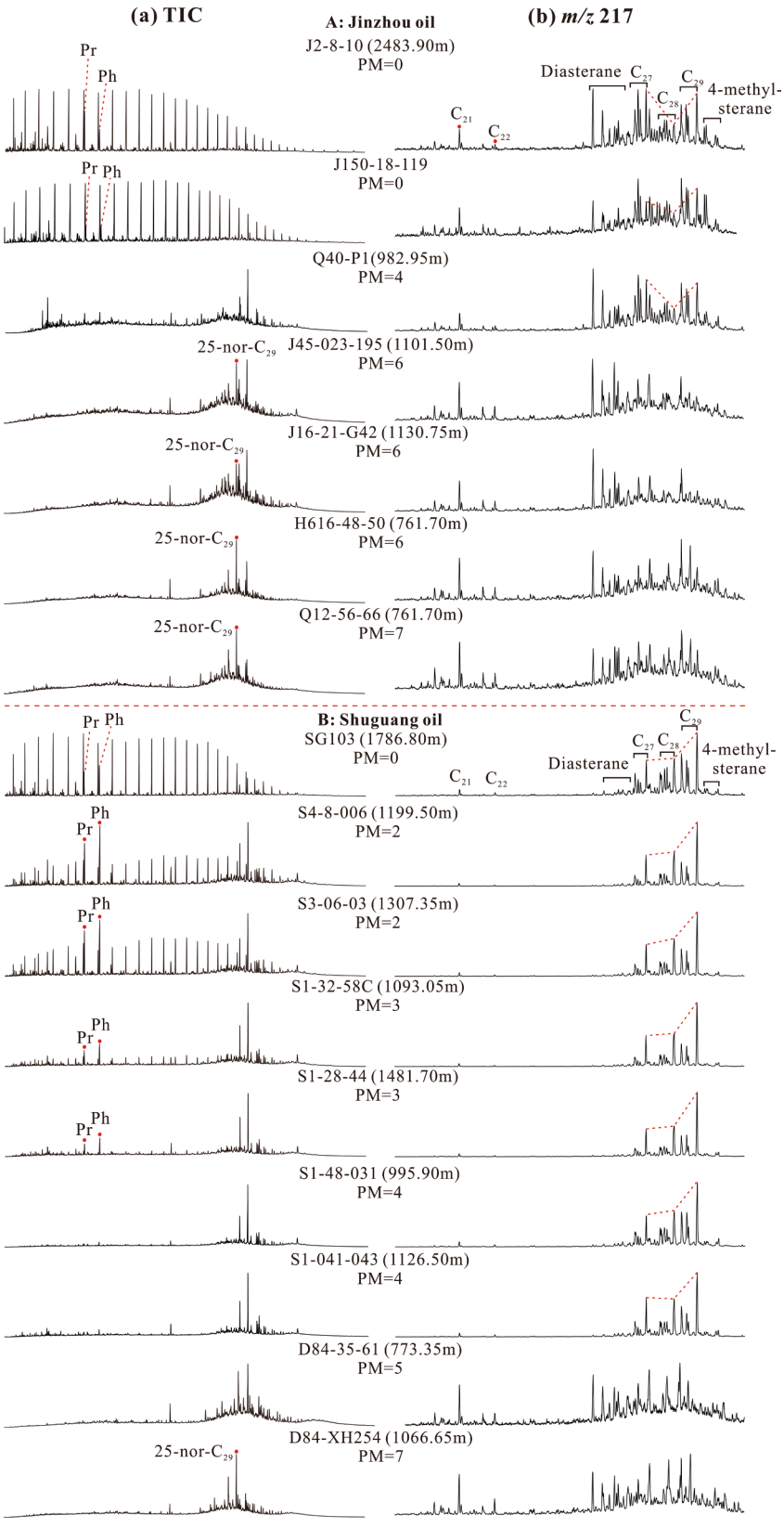

Fig. 2. (a) TIC and (b) m/z = 217 mass chromatograms of saturated hydrocarbon fractions.

source rocks of SG oils were deposited in a strongly reducing saline environment, with type I-II kerogen (Fig. S1a, b). The maturity levels of SG oils are relatively similar and fall within the low-maturity range (Fig. S1e). Our previous detailed oil-source rock correlation indicated that JZ oils primarily derived from the Es_3 source rock of freshwater origin in the Qingshui and Yuanyanggou sags, while SG oils mainly derive from Es_4 source rock of saline origin in the Panshan and Chenjia sags (Li et al., 2008).

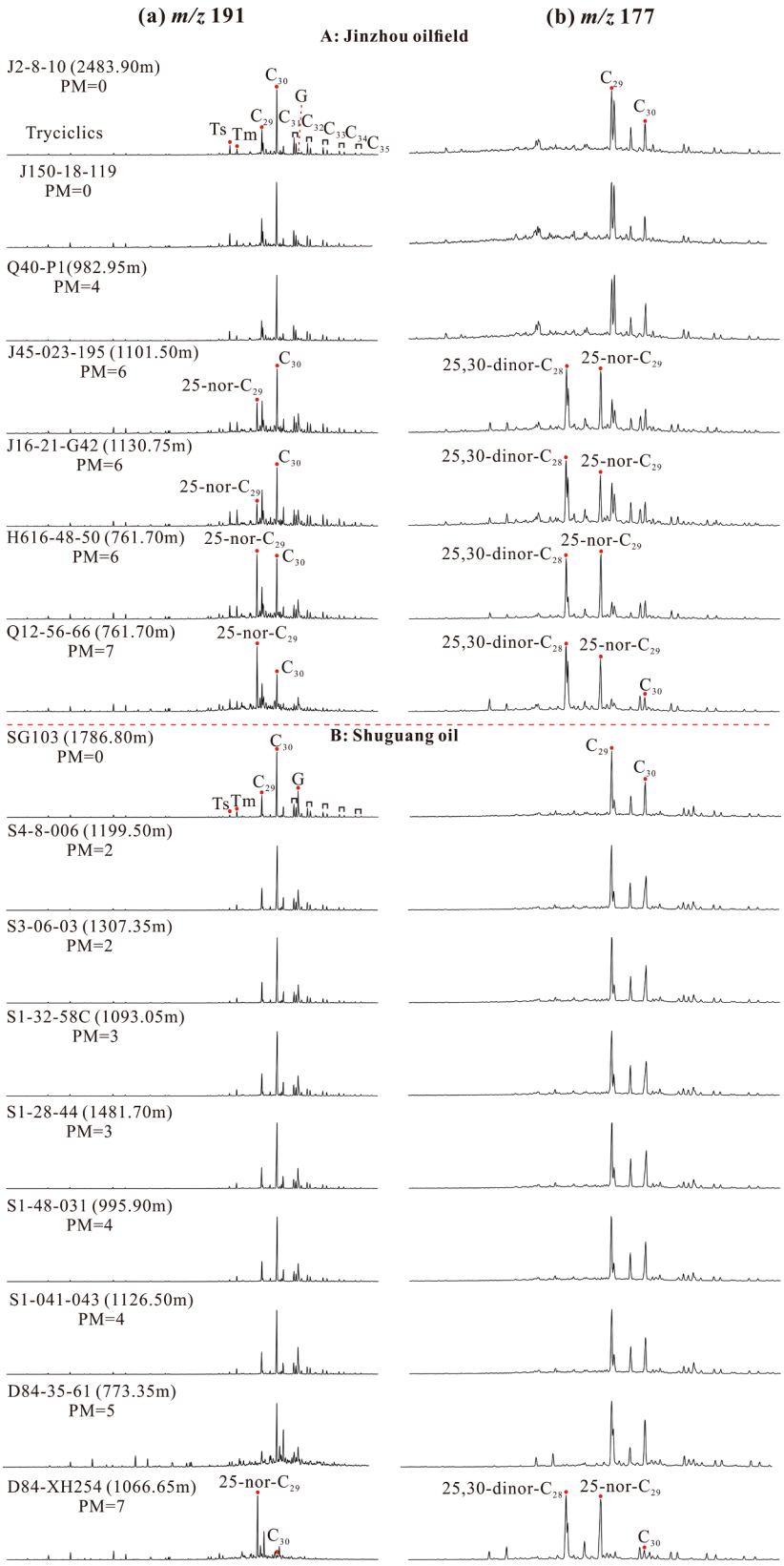

Fig. 3. (a) Mass chromatogram of *m/z* 191 and (b) *m/z* 177 for saturated hydrocarbon fractions.

4.3. ESI (−) FT-ICR MS characterization

4.3.1. Distribution of nitrogen- and oxygen-containing compounds

ESI (−) FT-ICR MS can be used to identify acidic oxygenates and non-basic nitrogenous compounds (Hughey et al., 2002; Hughey et al., 2004; Qian et al., 2001a). Seven types of heteroatom compounds, including N_1, N_1O_1, N_1O_2, O_1, O_2, O_3 and O_4, were detected in JZ and SG crude oils (Fig. 4). The nondegraded JZ oils (J2-8-10) is dominated by N_1 class

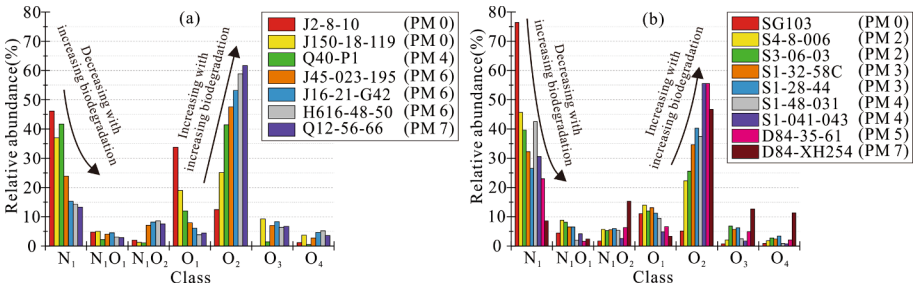

Fig. 4. Relative abundance of heteroatom class species in the oils as identified by ESI (−) FT-ICR MS.

species with a relative abundance of 46.10 %, followed by O_1 (33.75 %) and O_2 (12.46 %) class species, while the relative abundances of N_1O_1, N_1O_2, O_3 and O_4 class species are low (Table 2). Similarly, the non-degraded SG oil (SG103) is dominated by N_1 class species (76.41 %), followed by O_1 (11.05 %) and O_2 class species (5.05 %). Nondegraded SG oil (SG103) exhibits a significantly higher relative abundance of N_1 class species compared to nondegraded JZ oils (J2-8-10), while the relative abundances of O_1 and O_2 class species are lower than those in nondegraded JZ oils (Fig. 4b). The ESI (−) FT-ICR MS analysis reveals that saline lacustrine oils are enriched in N_1 class species. This result aligns with previous research from GC-MS analysis, where pyrrole compounds were more abundant in saline lacustrine oils compared to freshwater lacustrine oils (Clegg et al., 1997; Li et al., 1999). The observed characteristics are primarily related to a higher enrichment of sapropelic organic matter in saline lacustrine oil compared to freshwater lacustrine oil. Organic nitrogen-containing compounds are mainly derived from proteins, which are primarily enriched in aquatic plankton (Baxby et al., 1994). Terrestrial-sourced type III kerogen is known to contain a higher proportion of oxygen functional groups (Tissot and Welte, 1984), which can result in a lower relative abundance of N_1 class species.

As biodegradation intensifies, the relative abundance of N_1 class species gradually decreases, reaching 8.54 % to 23.88 % (average 16.36 %) in the PM = 5 ~ 7. The relative abundance of N_1O_1 slightly increases during the slight (PM = 1 ~ 3) degradation stages (4.99 %~8.79 %, average 6.98 %), whereas it declines during PM = 5 ~ 7 (1.62 %~4.45 %, average 3.04 %) (Fig. 4). This observation suggests that N_1O_1 may serve as an intermediate product in the N_1 biodegradation process (Kim et al., 2005; Liao et al., 2012). The relative abundance of N_1O_2 increases with the intensification of biodegradation (Fig. 4), suggesting that it may be a biodegradation product with the carboxyl group added to the pyrrole nucleus (de Aguiar et al., 2022; Vaz et al., 2013). The relative abundance of O_1 sharply decreases in the PM = 5 ~ 7 (3.26 %~7.87 %, average 5.33 %), which is consistent with previous observations (Kim et al., 2005). In contrast, the relative abundance of O_2 class species increases with the degree of biodegradation and becomes the predominant class species in the PM = 5 ~ 7 (46.69 %~61.73 %, average 53.93 %) (Fig. 4).

4.3.2. *Distribution of N_1 class species*

The nitrogen-containing compounds in crude oil primarily derive from plankton, bacteria and higher plants (Qian et al., 2001b). The protein content of plankton (>50 %) surpasses that of terrestrial higher plants. Moreover, other nitrogen-containing compounds like pigments and alkaloids are deemed to make minimal contributions to the sedimentary organic matter (Baxby et al., 1994). Consequently, the relative abundance of N_1 class species in SG oil (SG103), derived from type I kerogen is significantly higher than that in the JZ oil (J2-8-10), derived from type II~III kerogens (Fig. 4). N_1 class species ionized by the ESI (−) are neutral nitrogen-containing compounds with pyrrole structures (Hughey et al., 2002; Hughey et al., 2004; Qian et al., 2001a). The double bond equivalent (DBE) is a parameter utilized to quantify the number of double bonds and rings in a molecule. Both the JZ and SG oils exhibit DBE distributions ranging from 6 to 23, featuring prominent peaks at DBE = 9, 12 and 15 (Fig. 5). These peaks predominantly correspond to carbazole, benzocarbazole and dibenzocarbazole compounds, respectively (Hughey et al., 2007; Hughey et al., 2002; Hughey et al., 2004; Kim et al., 2005; Shi et al., 2010a; Shi et al., 2010b). In nondegraded samples, the relative abundance of DBE_9-N_1 (mainly carbazoles) in JZ oils with higher maturity is slightly lower than that in SG oils with low maturity (Fig. 6. a, d). This observation suggests that as crude oil matures, the degree of aromatization of nitrogenous

Table 2
The relative abundance of the classes and proxies analyzed by ESI (−) FT-ICR MS for the oils.

Well	PM	N_1	N_1O_1	N_1O_2	O_1	O_2	O_3	O_4	A	B	C	D
		%										
J2-8-10	0	46.10	4.72	1.91	33.75	12.46	0.00	1.06	0.98	2.74	1.78	0.16
J150-18-119	0	36.94	4.99	1.20	18.92	25.11	9.23	3.61	1.20	2.23	1.75	0.45
Q40-P1	4	41.70	2.12	0.96	11.95	41.44	1.38	0.44	1.15	0.26	0.40	0.77
J45-023-195	6	23.88	4.08	7.04	7.87	47.52	6.94	2.67	1.64	0.06	0.04	1.50
J16-21-G42	6	15.29	4.45	8.18	6.01	53.22	8.27	4.58	1.80	0.06	0.04	2.50
H616-48-50	6	14.22	2.96	8.54	3.81	58.90	6.41	5.16	2.11	0.06	0.05	3.27
Q12-56-66	7	13.23	2.80	7.57	4.41	61.73	6.69	3.56	2.07	0.05	0.03	3.50
SG103	0	76.41	4.38	1.62	11.05	5.05	0.69	0.81	0.79	3.73	3.69	0.06
S4-8-006	2	45.67	8.79	5.58	13.95	22.24	2.04	1.74	0.77	1.86	1.10	0.37
S3-06-03	2	39.64	8.10	5.27	11.99	25.51	6.82	2.67	0.86	1.70	1.30	0.49
S1-32-58C	3	32.25	6.51	5.56	13.05	34.65	5.68	2.30	1.02	0.56	0.52	0.76
S1-28-44	3	26.55	6.50	5.89	11.25	40.31	6.19	3.32	1.10	0.48	0.47	1.07
S1-48-031	4	42.56	1.94	5.38	9.44	37.39	2.46	0.83	1.10	0.23	0.25	0.72
S1-041-043	4	30.58	4.12	2.52	4.82	55.55	1.66	0.75	0.97	0.45	0.59	1.57
D84-35-61	5	23.00	1.62	6.31	6.60	55.53	4.88	2.06	1.64	0.09	0.07	1.88
D84-XH254	7	8.54	2.32	15.30	3.26	46.69	12.60	11.29	1.82	0.04	0.03	3.96

Note: A: $DBE_{(12+13+15)}/DBE_{9\sim11}$-$N_1$ (The ratio of the sum of DBE = 12, 13, 15 to that of the DBE = 9 ~ 11 of the N_1 species); B: A/C Ratio = DBE_1-$O_2/DBE_{2\sim4}$-O_2; C: Modified A/C Ratio 2 = DBE_1-$O_2/DBE_{3\sim6}$-O_2; D: $O_2/(N_1 + O_1)$.

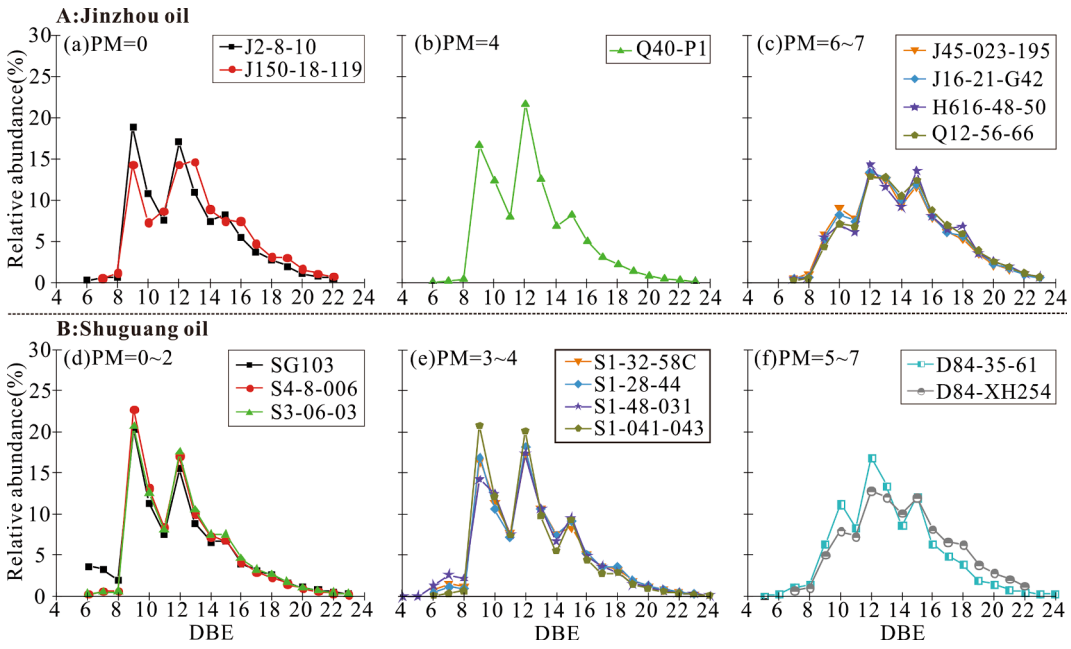

Fig. 5. Relative abundance of the N_1 class species with various DBE values in the crude oils detected by ESI (−) FT-ICR MS.

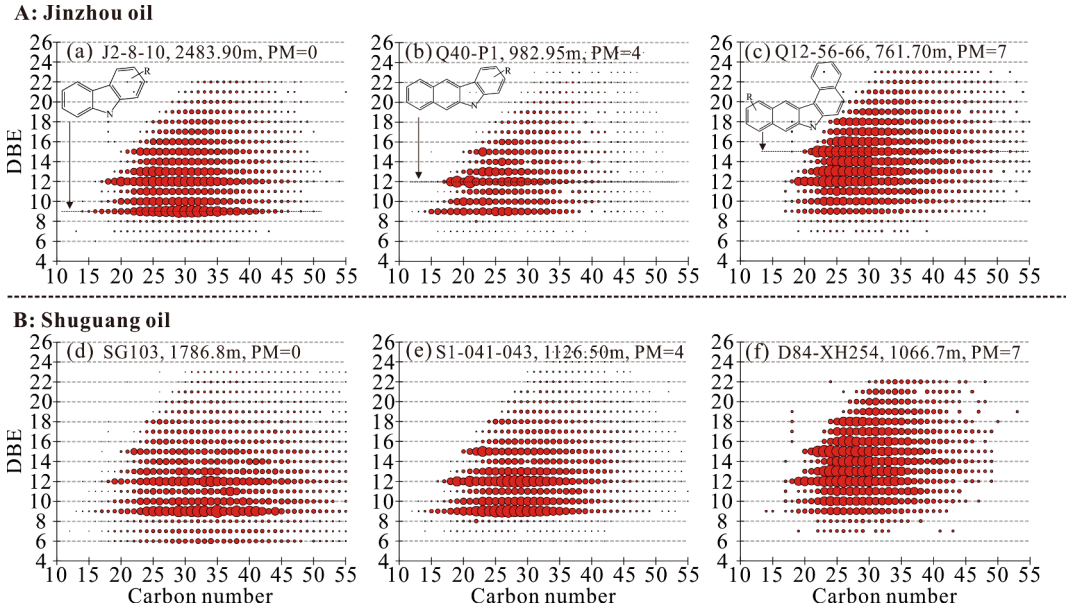

Fig. 6. Plots of DBE versus carbon number for the N_1 class species.

compounds increases (Ji et al., 2018; Oldenburg et al., 2014). The primary carbon number distribution ranges of N_1 class species in nondegraded JZ and SG oils are 17 ~ 45 and 16 ~ 53, respectively (Fig. 6a, d, Fig. S2). The difference is attributed to the relatively narrower carbon number range of N_1 class species in freshwater-phase crude oils (Ji et al., 2018) and the decrease in carbon number range with increasing maturity (Hughey et al., 2004; Ji et al., 2018; Wan et al., 2017).

With the increasing degree of biodegradation, the DBE values of N_1 increase (Fig. 5), the range of carbon number distribution decrease, the main peak carbon shifts towards lower values, and the abundance of high-carbon number compounds decrease (Fig. 6, Fig. S2). The relative abundance of DBE_9-N_1 (mainly carbazoles) gradually decreases, while the relative abundance of DBE_{12}-N_1 (mainly dibenzocarbazoles) increases and eventually replaces DBE_9-N_1 as the dominant compounds in the severely biodegraded stage (Fig. 5c, f). These observations indicate that N_1 class species with high degree of aromatization exhibit stronger resistance to biodegradation, while N_1 class species with longer alkyl side chains show weaker resistance to biodegradation. These results align with earlier research based on GC–MS (Huang et al., 2003; Sun et al., 2020) and FT ICR-MS (Kim et al., 2005; Liao et al., 2012; Sakai et al., 2021).

4.3.3. *Distribution of O_1 class species*

The DBE values of O_1 class species in nondegraded JZ and SG oils both range from 0 to 20, with DBE_4-O_1 being dominant (Fig. 7a, d). The main carbon number distribution ranges of JZ and SG crude oils is from 15 to 45 (Fig. 8a, d, Fig. S3). The presence of shorter alkyl side chains in JZ oils may be attributed to their higher maturity level (Ji et al., 2018). DBE_4-O_1 may correspond to alkylphenol compounds, while DBE_5-O_1 could be a compound containing both a phenolic structure and a cyclic

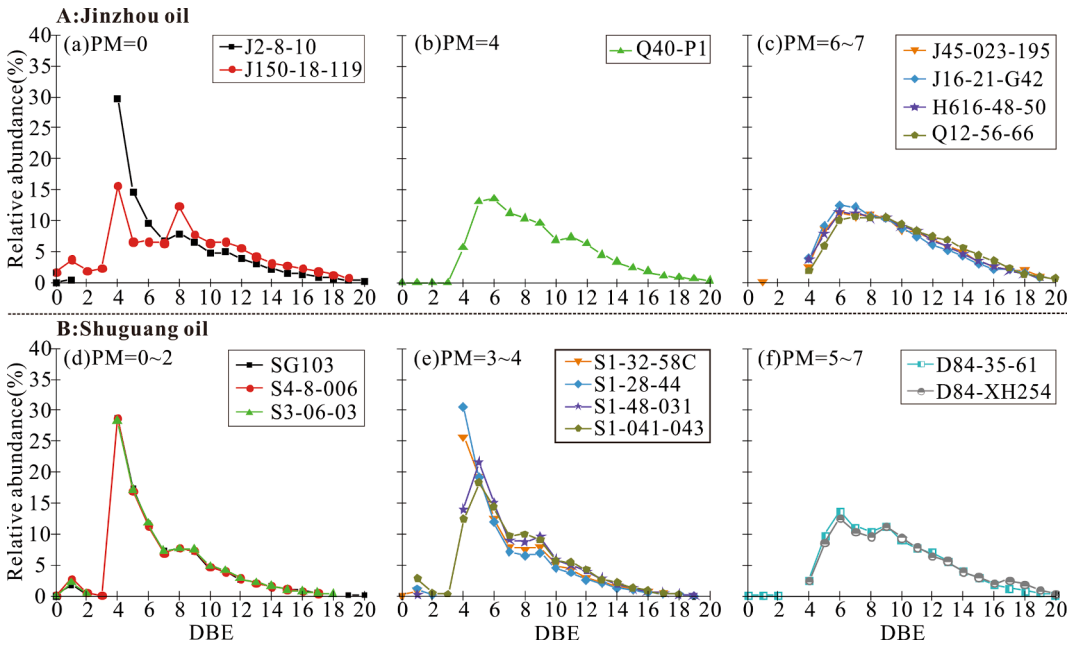

Fig. 7. Relative abundance of the O_1 class species with various DBE values in the crude oils detected by ESI (−) FT-ICR MS.

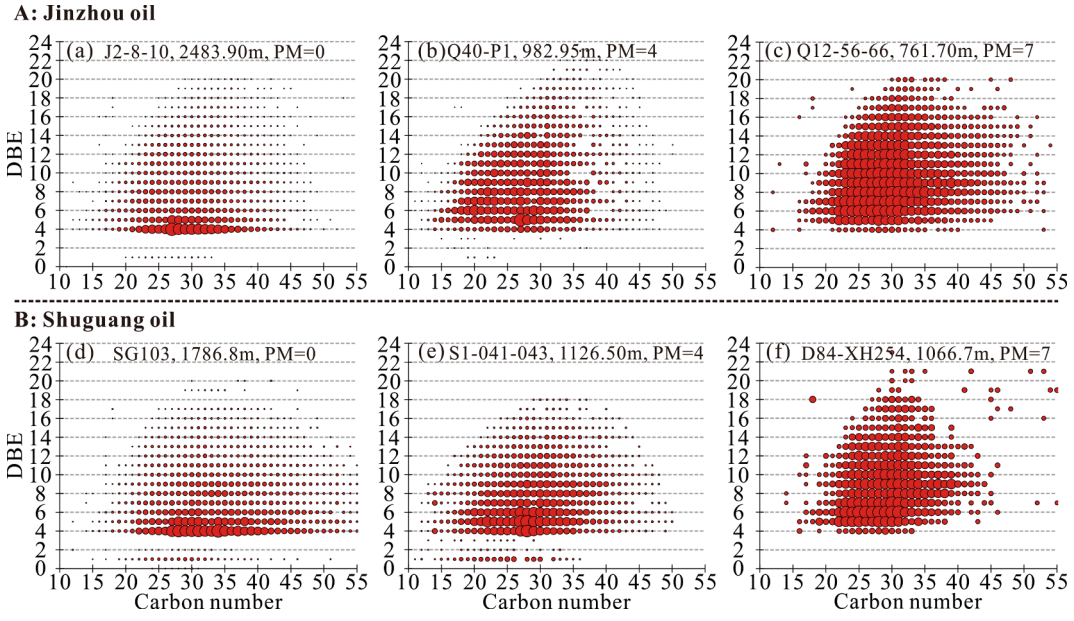

Fig. 8. Plots of DBE versus carbon number for the O_1 class species.

alkane ring (Kim et al., 2005; Liao et al., 2012). Nondegraded JZ oils display a higher relative abundance of O_1 class species compared to the SG oils (Fig. 4), indicating that this difference is primarily influenced by the source kerogen type (a mixture of type II~III and type I~II kerogen, respectively) (Bastow et al., 2003; Ji et al., 2018; Wan et al., 2017).

A small amount of DBE_1-O_1 compounds were detected in the non-degraded oils. These compounds are alcohol compounds (Kamga et al., 2014; Shi et al., 2010a), which are intermediate products produced by the terminal oxidation of alkanes (Das and Chandran, 2011; Greenwood et al., 2008) or functioning as intermediary products during the conversion of organic matter to hydrocarbons (Amrani and Aizenshtat, 2004; Rojas-Ruiz and Orrego-Ruiz, 2016). These compounds completely disappear in the stage of severe degradation (Fig. 7c, f). The content of DBE_4-O_1 (alkylphenol compounds) is predominant in nondegraded oils (Fig. 7a, d). During moderate degradation stage, their content remains relatively stable (Fig. 7e), while in the severe degradation stage, they are almost completely depleted (Fig. 7c, f). This phenomenon indicates that DBE_4-O_1 compounds can be degraded by microorganisms. However, in the early stages of biodegradation (PM $<$ 4), the DBE_4-O_1 compounds may also serve as intermediate products in the anaerobic degradation of aromatic compounds (Grbić-Galić and Vogel, 1987; Harwood et al., 1998; Vogel and Grbìc-Galìc, 1986). The relative abundance of compounds with DBE $>$ 6 slightly increases with the degree of degradation (Fig. 7), indicating that phenols with naphthenic rings are more resistant to biodegradation than alkylphenols, and O_1 compounds with a higher degree of condensation exhibit stronger resistance to biodegradation. These observations are consistent with previous research findings (Liu et al., 2020; Meredith et al., 2000; Oldenburg et al., 2017).

4.3.4. Distribution of O_2 class species

Organic acids present in nondegraded oil are derive kerogen degradation. These acids are typically minor components in most crudes, but can be significantly more abundant in very low maturity oils (Mackenzie et al., 1983; Peters et al., 2005). The biodegradation of crude oil primarily involves the oxidation of hydrocarbons, resulting in the production of CO_2 and partially oxidezed compounds, including organic acids (Peters et al., 2005). Acids are readily formed during biodegradation processes in the reservoir, indicating that biodegradation plays a significant role in the formation of high acid crude oil (Shi et al., 2010b). O_2 class species, commonly regarded as carboxylic acids, are abundant in low maturity and biodegraded oils (Headley et al., 2016; Shi et al., 2010b). The DBE distribution range of O_2 class species in the nondegraded/slight degradation JZ and SG crude oils is 0 ~ 19, with DBE = 1 being predominant (Fig. 9a, d). The carbon number distribution ranges are 11 ~ 45 (mainly 15 ~ 45) and 11 ~ 53 (mainly 15 ~ 45), respectively (Fig. 10a, d). O_2 class species with DBE = 1 are likely to be fatty acids, and O_2 class species with DBE = 2 ~ 7 correspond to naphthenic acids with 1 ~ 6-cyclic (Kim et al., 2005; Shi et al., 2010b). Normal alkanes may serve as precursors for fatty acids (El-Sabagh and Al-Dhafeer, 2000). A close relationship exists between fatty acids with low thermal stability and the formation of low-maturity oils (Ji et al., 2018; Shi et al., 2001). The abundance of DBE_1-O_2 in nondegraded saline lacustrine low maturity oil (SG103) is significantly higher than that of nondegraded freshwater lacustrine mature oil (J2-8-10) (Fig. 9a, d), indicating that both maturity and depositional environment/organic matter sources may have complex effects on heteroatomic compounds (Ji et al., 2018; Rocha et al., 2018; Wan et al., 2017).

With the increasing degree of biodegradation, the content of fatty acids decreases significantly and almost disappears in the severely biodegraded stage (Fig. 9), indicating that fatty acids have the weakest resistance to biodegradation among the O_2 class species. The relative abundance of mononaphthenic acids (DBE = 2) shows a slight increase in the slight to moderate degradation stages but decreases significantly in the heavy to severe degradation stage (Fig. 9), suggesting that 1-cyclic naphthenic acids exhibit relatively weak resistance to biodegradation (Martins et al., 2017). The relative abundance of 2 ~ 3-cyclic naphthenic acids (DBE = 3 ~ 4) increases with the degree of biodegradation (Fig. 9b, e) and becomes the predominant acids in the severe degradation stage, surpassing the abundance of 4 ~ 5-cyclic naphthenic acids (DBE = 5 ~ 6) (Fig. 9c, f). This observation aligns with the findings of Kim et al. (2005) and Cheng and Hou (2021) and indicates that 2 ~ 3-cyclic naphthenic acids possess higher resistance to biodegradation (Liao et al., 2012), or their net production rate is faster in the severe degradation stage. The DBE_5-O_2 and DBE_6-O_2 are mainly naphthenic acids with specific biological skeletons. Among them, $C_{27\sim30}$-DBE_5-O_2 corresponds mainly to steranic acids, and $C_{29\sim35}$-DBE_6-O_2 corresponds mainly to hopanic acids (Kim et al., 2005; Poetz et al., 2014; Shi et al., 2010a; Shi et al., 2010b). During the thermal evolution process, decarboxylation reactions transform them into steranes and hopanes, respectively (Farrimond et al., 2002; Poetz et al., 2014). Our results show that with the increasing degree of biodegradation, the abundance of $C_{27\sim30}$-DBE_5-O_2 (mainly steranic acids) and $C_{29\sim35}$-DBE_6-O_2 (mainly hopanic acids) gradually increases (Fig. 9). During the aerobic biodegradation of crude oil, hopanes can be transformed into hopanic acids through side-chain oxidation (Kim et al., 2005; Liao et al., 2012; Meredith et al., 2000), but the biodegradation pathway of steranes is still unclear. Hopanoic acids is produced by specific degradative bacteria, and significant shifts in their distribution indicate alterations in the microbial degradation pathway (Hughey et al., 2007; Kim et al., 2005). In the slight to heavy biodegradation stage, there is a relative enrichment of C_{30} ~ C_{32} hopanoic acids (Fig. 10d, e). On the contrary, the content of hopanoic acids with other carbon numbers increases in the severe degradation stage (Fig. 10c, f). This suggests that degradative bacteria produce a significant amount of hopanoic acids, and the microbial population changes. Biodegradation affects hopanoic acid with varying carbon numbers through distinct pathways (Hughey et al., 2007; Kim et al., 2005).

5. Biodegradation evaluation by ESI (−) FT-ICR MS

5.1. Based on N_1 class species

N_1 class species can be utilized to assess the maturity of crude oils and source rock (Hughey et al., 2004; Ji et al., 2018; Oldenburg et al., 2014; Poetz et al., 2014; Wan et al., 2017), as well as to track the migration pathways of hydrocarbon (Liu et al., 2015; Zhang et al., 2016; Ziegs et al., 2018). However, they are seldom applied for evaluating biodegradation. Previous studies have indicated that N_1 class species with more condensed ring structures exhibit higher resistance to

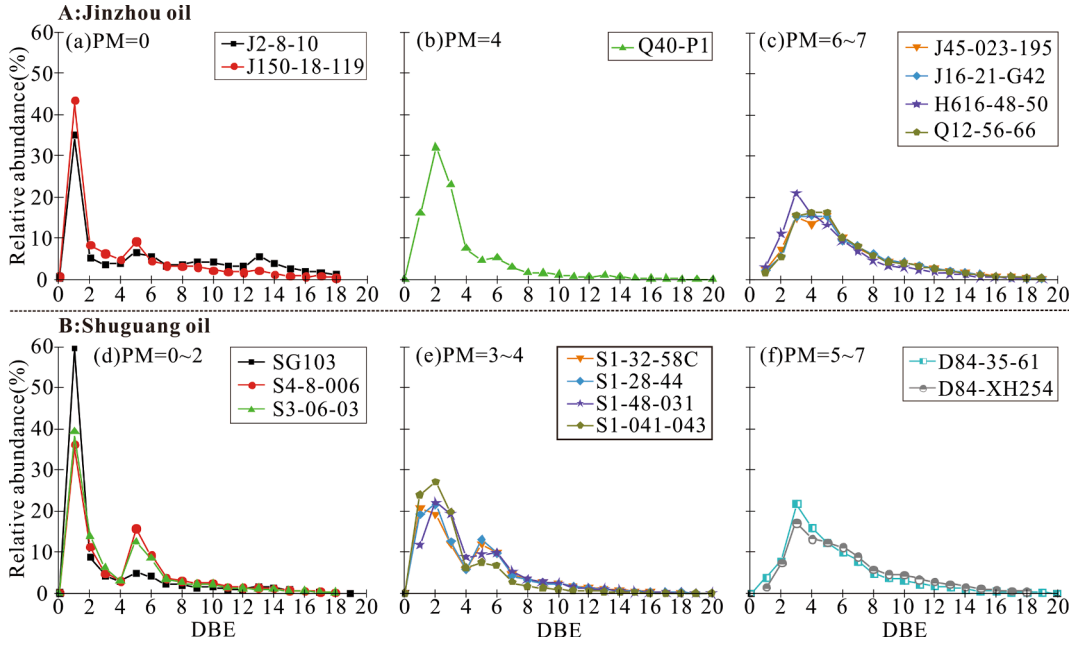

Fig. 9. Relative abundance of the O_2 class species with various DBE values in the crude oils detected by ESI (−) FT-ICR MS.

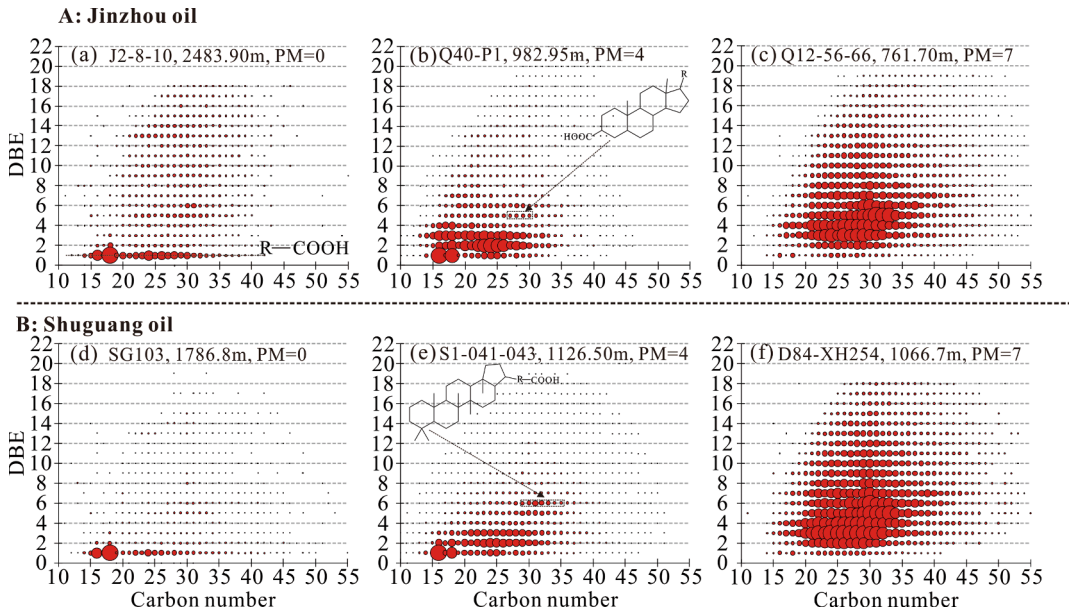

Fig. 10. Plots of DBE versus carbon number for the O_2 class species.

biodegradation (Liao et al., 2012; Pan et al., 2017). Therefore, a ternary graph of the relative abundance of DBE_9-N_1, DBE_{12}-N_1, and DBE_{15}-N_1 has been proposed as a tool for assessing the degree of biodegradation in crude oil (Oldenburg et al., 2017). However, this proxy may not be effective in determining the degree of degradation in severely biodegraded crude oil. Results from this study demonstrate that biodegradation leads to a decrease in the relative abundance of N_1 class species (Fig. 4), an increase in DBE values and an enrichment of compounds with higher DBE values (Fig. 5). Additionally, it leads to a reduction in the range of carbon number distribution and a decrease in the abundance of compounds with high carbon numbers (Fig. 6). Based on the observation that the DBE values increase with the enhancement of biodegradation, we proposed the proxies $DBE_{12,\ 13,\ 15}/DBE_{9\sim11}$-$N_1$ (Proxy A, Table 2) to represent the ratio of N_1 class species with high and low DBE values. It is observed that the $DBE_{12,\ 13,\ 15}/DBE_{9\sim11}$-$N_1$ values of the same type crude oil exhibit a robust correlation with the PM scale, with correlation coefficients (r) of 0.88 and 0.89, respectively (Fig. 11a). The density of crude oil typically increases with the enhancement of biodegradation (Connan, 1984). Similarly, the $DBE_{12,\ 13,\ 15}/DBE_{9\sim11}$-$N_1$ values of JZ and SG oils exhibit a robust correlation with density, having correlation coefficients (r) of 0.77 and 0.81, respectively (Fig. 11b). Therefore, the mentioned proxy can be applied to assess the degree of biodegradation in crude oil, encompassing slight to severe degradation. Notably, the degree of condensation of N_1 class species tends to rise, with an increase in maturity (Hughey et al., 2004; Ji et al., 2018; Wan et al., 2017). Consequently, the $DBE_{12,13,15}/DBE_{9\sim11}$-$N_1$ values of the higher maturity JZ oils exhibit slightly higher values compared to those of the SG oils (Fig. 11a).

5.2. *Based on O_2 class species*

ESI FT-ICR MS has been extensively employed in studying O_2 class species in biodegraded crude oil (Hughey et al., 2007; Hughey et al., 2008; Kim et al., 2005; Li et al., 2010a; Liao et al., 2012; Pan et al., 2013; Shi et al., 2010b). Kim et al. (2005) proposed using the ratio of acyclic fatty acids to 1 ~ 3-cyclic naphthenic acids (A/C Ratio = DBE_1-O_2/$DBE_{2\sim4}$-O_2) (Proxy B, Table 2) as a proxy for evaluating the degree of biodegradation in crude oils. The proxy effectively assesses the degree of biodegradation in homogeneous or even non-homogeneous crude oils with slight to moderate degradation (Martins et al., 2017; Vaz et al., 2013). However, its accuracy is limited when dealing with severely biodegraded crude oils (Angolini et al., 2015; Hughey et al., 2007). To validate the effectiveness of the proxy, the A/C Ratios of the samples were applied into the trendline formula proposed by Kim et al. (2005) and the Acid Biodegradation Index values calculated. The observation revealed that the A/C Ratio generally underestimated the degree of biodegradation, particularly for moderate and severely biodegraded oils (Fig. 12a). We demonstrated that biodegradation led to a decrease in the content of acyclic fatty acids and an increase in the content of 2 ~ 5-cyclic naphthenic acids. Notably, the relative abundance of 1-cyclic

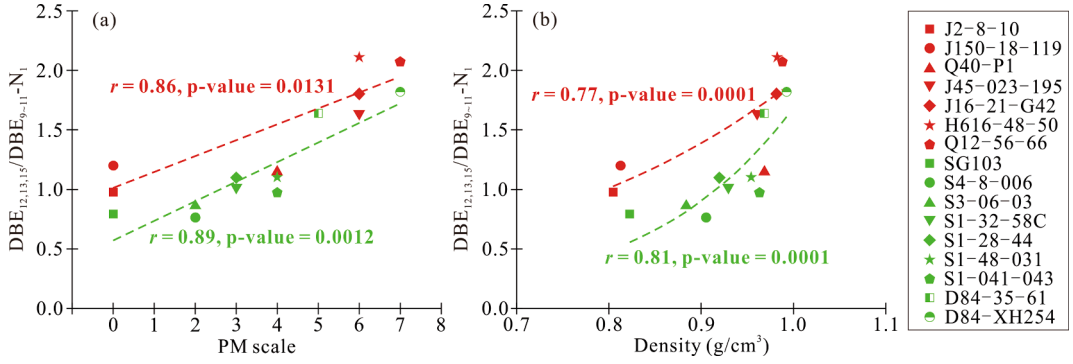

Fig. 11. (a) Cross plot of the $DBE_{12,\ 13,\ 15}/DBE_{9\sim11}$-$N_1$ versus the PM scale; (b) Cross plot of the $DBE_{12,\ 13,\ 15}/DBE_{9\sim11}$-$N_1$ versus density.

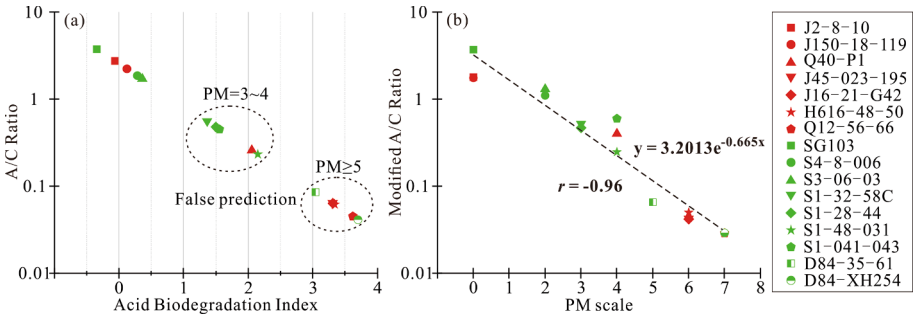

Fig. 12. Comparison of two biodegradation indices: (a) The Acid Biodegradation Index proposed by Kim et al. (2005) is based on the ratio of acyclic to cyclic acids (A/C Ratio); (b) The correlation between the Modified A/C Ratio 2 and the PM scale.

naphthenic acids (DBE_2-O_2) exhibited a slight increase in the slight to moderate degradation stages but showed a significantly decreased in the severe degradation stage (Fig. 9). Therefore, we suggest that the relatively weak resistance of 1-cyclic naphthenic acids to biodegradation might be the primary reason for the failure of the A/C Ratio. Due to the continuous increase in the abundance of 2 ~ 5-cyclic naphthenic acids ($DBE_{3\sim6}$-O_2) with the enhancement of biodegradation (Fig. 9), we propose a new proxy, the Modified A/C Ratio 2 (DBE_1-O_2/$\sum DBE_{3\sim6}$-O_2) (Proxy C, Table 2), as the ratio of the relative abundance of acyclic fatty acids to the sum of 2 ~ 5-cyclic naphthenic acids. This proxy exhibits a strong correlation with the PM scale from nondegraded to severely degraded stage (r = -0.97) (Fig. 12b). It serves as a valuable tool in assessing biodegradation, compensating for the limitations of previous studies in which similar proxy failed to effectively assess severe degradation stages (Kim et al., 2005; Martins et al., 2017; Vaz et al., 2013).

5.3. Based on bulk composition and abundance of NOs compound

As the degree of biodegradation increases, certain compounds in the crude oil (e.g., O_1 class species) undergo oxidation to produce a substantial quantity of acids (O_2 class species), resulting a dilution or reduction in the relative abundance of other compound classes (e.g., N_1 class species) (Kim et al., 2005). An increase in the content of heteroatomic compounds represented by acids in crude oil frequently results in an increase in its density (Connan, 1984). According to the aforementioned characteristics, we propose a new proxy $O_2/(N_1 + O_1)$ Ratio (Proxy D, Table 2), which can be applied to indicate the formation of acids in the crude oil during the biodegradation process. This proxy exhibits a robust positive correlation with both crude oil density and PM scale (r = 0.95 and 0.95, respectively) (Fig. 13). The $O_2/(N_1 + O_1)$ Ratios of crude oils with similar degrees of degradation but different origins and maturities (e.g., J2-8-10 and SG103, Q12-56-66 and D84-XH254) show relatively little differences (<0.46) (Fig. 13b). Therefore, we conclude that the $O_2/(N_1 + O_1)$ Ratio is less influenced by organic matter type or maturity, and biodegradation is the primary controlling factor for this proxy. The proxy can accurately and quantitatively identify the degree of biodegradation, ranging from nondegraded to severely biodegraded crude oils. However, it is important to clarify that this proxy presently pertains exclusively to lacustrine oils (both saline and freshwater). Given the notable discrepancies in heteroatomic compounds between marine and lacustrine oils (Rocha et al., 2018), it is imperative to verify the suitability of this proxy for marine oil samples.

6. Conclusions

Biodegradation significantly influences the distribution of heteroatomic compounds in crude oil. As the degree of biodegradation increases, the abundance of O_2 class species significantly increases, while the abundance of O_1 and N_1 class species decreases. O_2 class species become the dominant compounds in the severe degradation stage.

N_1 class species with higher DBE values demonstrate greater resistance to biodegradation, resulting in an increase in their relative abundance during the process. In contrast, those with lower DBE values experience a decrease in relative abundance. Hence, the proxy of N_1 class species ($DBE_{12,13,15}$/$DBE_{9\sim11}$-N_1) can be utilized to assess the biodegradation level of crude oils with comparable maturity.

The significant decrease in the relative abundance of 1-cyclic naphthenic acids during severe degradation renders the A/C Ratio (DBE_1-O_2/$DBE_{2\sim4}$-O_2) ineffective in accurately assessing samples undergoing such degradation. Consequently, we introduce the Modified A/C Ratio 2 (DBE_1-O_2/$\sum DBE_{3\sim6}$-O_2), which demonstrates a strong correlation with the PM scale from nondegraded to severely degraded. A new proxy, the $O_2/(N_1 + O_1)$ Ratio is indicative of acids formation during the biodegradation process, showing a robust positive correlation with both crude oil density and the PM scale. The above two proxies effectively quantify biodegradation levels from nondegraded to severely degraded oils of different depositional environments/sources and maturities.

The new proxies have broader applicability and can effectively complement the PM scale, enabling a more refined quantitative evaluation of crude oil biodegradation. The ESI FT-ICR MS technique is of great value in the evaluation of heavy oil and the study of formation mechanisms.

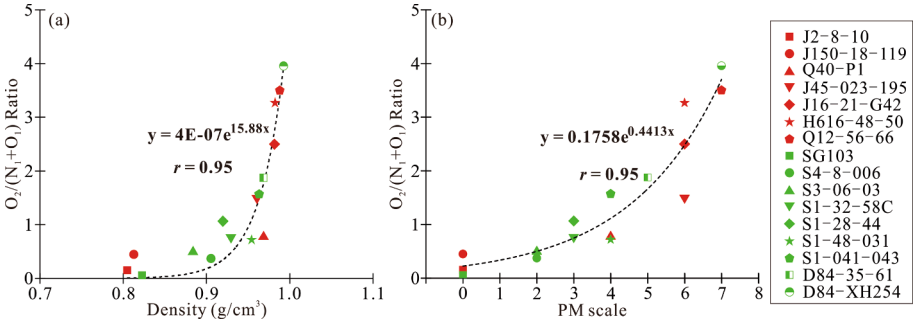

Fig. 13. (a) Cross plot of the $O_2/(N_1 + O_1)$ species versus density; (b) The correlation between the $O_2/(N_1 + O_1)$ Ratio and the PM scale.

CRediT authorship contribution statement

Shuo Deng: Writing – original draft, Visualization, Validation, Software, Methodology, Investigation, Data curation, Conceptualization. **Sumei Li:** Writing – review & editing, Supervision, Resources, Project administration. **Xiaoyan Li:** Investigation.

Declaration of competing interest

The authors declare that they have no known competing financial interests or personal relationships that could have appeared to influence the work reported in this paper.

Acknowledgement

This study was funded by the National Natural Science Foundation of China (Grant Nos. # 42073064; # 41673055). The authors are grateful for the assistance of State Key Laboratory of Heavy Oil of China University of Petroleum for the FT-ICR MS analyses. We would also like to thank Yuhong Liao and two anonymous reviewers for the helpful comments.

Appendix A. Supplementary material

Supplementary data to this article can be found online at https://doi.org/10.1016/j.orggeochem.2024.104815.

References

Adams, J., Jiang, C., Bennett, B., Huang, H., Oldenburg, T., Noke, K., Snowdon, L., Gates, I., Larter, S., 2008. Viscosity determination of heavy oil and bitumen; World Heavy Oil Congress, March 9–12. Edmonton, Canada, Paper 2008–2443.

Amrani, A., Aizenshtat, Z., 2004. Photosensitized oxidation of naturally occurring isoprenoid allyl alcohols as a possible pathway for their transformation to thiophenes in sulfur rich depositional environments. Organic Geochemistry 35, 693–712.

Angolini, C.F.F., Capilla, R., Marsaioli, A.J., 2015. Petroleum biodegradation effects on polar acidic compounds and correlation with their corresponded hydrocarbon fractions. Energy & Fuels 29, 4886–4892.

Bastow, T.P., van Aarssen, B.G.K., Herman, R., Alexander, R., Kagi, R.I., 2003. The effect of oxidation on the distribution of alkylphenols in crude oils. Organic Geochemistry 34, 1103–1111.

Baxby, M., Patience, R.L., Bartle, K.D., 1994. The origin and diagenesis of sedimentary organic nitrogen. Journal of Petroleum Geology 17, 211–230.

Chen, X.Z., Shao, J.X., Sun, Z., Han, H.W., Guo, Q., Yin, Y.P., Sun, X.Y., 2023. Characteristics and controlling factors of heavy oil distribution in Liaohe Depression, Bohai Bay Basin. Petroleum Geology & Experiment 45, 317–326.

Cheng, X., Hou, D.J., 2021. Characterization of severely biodegraded crude oils using negative-ion ESI Orbitrap MS, GC-NCD and GC-SCD: Insights into heteroatomic compounds biodegradation. Energies 14, 300.

Clegg, H., Wilkes, H., Horsfield, B., 1997. Carbazole distributions in carbonate and clastic source rocks. Geochimica et Cosmochimica Acta 61, 5335–5345.

Connan, J., 1984. Biodegradation of crude oils in reservoirs. In: Brook, J., Welte, D. (Eds.), Advances in Petroleum Geochemistry 1. Academic Press, pp. 229–335.

Connan, J., Cassou, A.M., 1980. Properties of gases and petroleum liquids derived from terrestrial kerogen at various maturation levels. Geochimica et Cosmochimica Acta 44, 1–23.

Das, N., Chandran, P., 2011. Microbial degradation of petroleum hydrocarbon contaminants: An overview. Biotechnology Research International 2011, 941810.

de Aguiar, D.V.A., da Silva Lima, G., da Silva, R.R., Júnior, I.M., Gomes, A.d.O., Mendes, L.A.N., Vaz, B.G., 2022. Comprehensive composition and comparison of acidic nitrogen- and oxygen-containing compounds from pre- and post-salt Brazilian crude oil samples by ESI (-) FT-ICR MS. Fuel 326, 125129.

Derenne, S., Largeau, C., Berkaloff, C., Rousseau, B., Wilhelm, C., Hatcher, P.G., 1992. Non-hydrolysable macromolecular constituents from outer walls of *Chlorella fusca* and *Nanochlorum eucaryotum*. Phytochemistry 31, 1923–1929.

Difan, H., Jinchao, L., Dajiang, Z., 1990. Maturation sequence of continental crude oils in hydrocarbon basins in China and its significance. Organic Geochemistry 16, 521–529.

El-Sabagh, S.M., Al-Dhafeer, M.M., 2000. Occurrence and distribution of *n*-alkanesand *n*-fatty acids in Saudi Arabian crude oils. Petroleum Science and Technology 18, 743–754.

Farrimond, P., Griffiths, T., Evdokiadis, E., 2002. Hopanoic acids in Mesozoic sedimentary rocks: Their origin and relationship with hopanes. Organic Geochemistry 33, 965–977.

Grantham, P.J., 1986. The occurence of unusual C_{27} and C_{29} sterane predominances in two types of Oman crude oil. Organic Geochemistry 9, 1–10.

Grbić-Galić, D., Vogel, T.M., 1987. Transformation of toluene and benzene by mixed methanogenic cultures. Applied and Environmental Microbiology 53, 254–260.

Greenwood, P.F., Wibrow, S., George, S.J., Tibbett, M., 2008. Sequential hydrocarbon biodegradation in a soil from arid coastal Australia, treated with oil under laboratory controlled conditions. Organic Geochemistry 39, 1336–1346.

Harwood, C.S., Burchhardt, G., Herrmann, H., Fuchs, G., 1998. Anaerobic metabolism of aromatic compounds via the benzoyl-CoA pathway. FEMS Microbiology Reviews 22, 439–458.

Headley, J.V., Peru, K.M., Barrow, M.P., 2016. Advances in mass spectrometric characterization of naphthenic acids fraction compounds in oil sands environmental samples and crude oil—A review. Mass Spectrometry Reviews 35, 311–328.

Hein, F.J., 2017. Geology of bitumen and heavy oil: An overview. Journal of Petroleum Science and Engineering 154, 551–563.

Huang, H., Bowler, B.F.J., Zhang, Z., Oldenburg, T.B.P., Larter, S.R., 2003. Influence of biodegradation on carbazole and benzocarbazole distributions in oil columns from the Liaohe basin, NE China. Organic Geochemistry 34, 951–969.

Huang, H., Bowler, B.F.J., Oldenburg, T.B.P., Larter, S.R., 2004. The effect of biodegradation on polycyclic aromatic hydrocarbons in reservoired oils from the Liaohe basin, NE China. Organic Geochemistry 35, 1619–1634.

Hughes, W.B., Holba, A.G., Dzou, L.I.P., 1995. The ratios of dibenzothiophene to phenanthrene and pristane to phytane as indicators of depositional environment and lithology of petroleum source rocks. Geochimica et Cosmochimica Acta 59, 3581–3598.

Hughey, C.A., Rodgers, R.P., Marshall, A.G., Qian, K.N., Robbins, W.K., 2002. Identification of acidic NSO compounds in crude oils of different geochemical origins by negative ion electrospray Fourier transform ion cyclotron resonance mass spectrometry. Organic Geochemistry 33, 743–759.

Hughey, C.A., Rodgers, R.P., Marshall, A.G., Walters, C.C., Qian, K.N., Mankiewicz, P., 2004. Acidic and neutral polar NSO compounds in Smackover oils of different thermal maturity revealed by electrospray high field Fourier transform ion cyclotron resonance mass spectrometry. Organic Geochemistry 35, 863–880.

Hughey, C.A., Galasso, S.A., Zumberge, J.E., 2007. Detailed compositional comparison of acidic NSO compounds in biodegraded reservoir and surface crude oils by negative ion electrospray Fourier transform ion cyclotron resonance mass spectrometry. Fuel 86, 758–768.

Hughey, C.A., Minardi, C.S., Galasso-Roth, S.A., Paspalof, G.B., Mapolelo, M.M., Rodgers, R.P., Marshall, A.G., Ruderman, D.L., 2008. Naphthenic acids as indicators of crude oil biodegradation in soil, based on semi-quantitative electrospray ionization Fourier transform ion cyclotron resonance mass spectrometry. Rapid Communication of Mass Spectrometry 22, 3968–3976.

Ji, H., Li, S.M., Greenwood, P., Zhang, H.G., Pang, X.Q., Xu, T.W., He, N.N., Shi, Q., 2018. Geochemical characteristics and significance of heteroatom compounds in lacustrine oils of the Dongpu Depression (Bohai Bay Basin, China) by negative-ion Fourier transform ion cyclotron resonance mass spectrometry. Marine and Petroleum Geology 97, 568–591.

Kamga, A.W., Behar, F., Hatcher, P.G., 2014. Quantitative analysis of long chain fatty acids present in a type I kerogen using electrospray ionization Fourier transform ion cyclotron resonance mass spectrometry: Compared with BF_3/MeOH Methylation/GC-FID. Journal of the American Society for Mass Spectrometry 25, 880–890.

Kim, S., Stanford, L.A., Rodgers, R.P., Marshall, A.G., Walters, C.C., Qian, K., Wenger, L. M., Mankiewicz, P., 2005. Microbial alteration of the acidic and neutral polar NSO compounds revealed by Fourier transform ion cyclotron resonance mass spectrometry. Organic Geochemistry 36, 1117–1134.

Larter, S., Huan, H., Adams, J., Bennett, B., Jokanola, O., Oldenburg, T., Jones, M., Head, I., Riediger, C., Fowler, M., 2006. The controls on the composition of biodegraded oils in the deep subsurface: Part II - Geological controls on subsurface biodegradation fluxes and constraints on reservoir-fluid property prediction. AAPG Bulletin 90, 921–938.

Larter, S., Huang, H., Adams, J., Bennett, B., Snowdon, L.R., 2012. A practical biodegradation scale for use in reservoir geochemical studies of biodegraded oils. Organic Geochemistry 45, 66–76.

Li, M., Cheng, D., Pan, X., Dou, L., Hou, D., Shi, Q., Wen, Z., Tang, Y., Achal, S., Milovic, M., Tremblay, L., 2010a. Characterization of petroleum acids using combined FT-IR, FT-ICR–MS and GC–MS: Implications for the origin of high acidity oils in the Muglad Basin, Sudan. Organic Geochemistry 41, 959–965.

Li, S.M., Pang, X.Q., Liu, K.Y., Gao, X.Z., Li, X.G., Chen, Z.Y., Liu, B.H., 2008. Formation mechanisms of heavy oils in the Liaohe Western Depression, Bohai Gulf Basin. Science in China Series D-Earth Sciences 51, 156–169.

Li, S.M., Pang, X.Q., Jin, Z.J., Yang, H.J., Xiao, Z.Y., Gu, Q.Y., Zhang, B.S., 2010b. Petroleum source in the Tazhong Uplift, Tarim Basin: New insights from geochemical and fluid inclusion data. Organic Geochemistry 41, 531–553.

Li, S.M., Wang, T.G., Zhang, A.Y., Guo, S.H., Zhang, S.C., 1999. Geochemistry characteristics and significane of the pyrrolic compounds in petroleum. Acta Sedimentologica Sinica 147–152 (in Chinese with English abstract).

Liao, Y.H., Shi, Q., Hsu, C.S., Pan, Y.H., Zhang, Y.H., 2012. Distribution of acids and nitrogen-containing compounds in biodegraded oils of the Liaohe Basin by negative ion ESI FT-ICR MS. Organic Geochemistry 47, 51–65.

Liu, P., Li, M., Jiang, Q., Cao, T., Sun, Y., 2015. Effect of secondary oil migration distance on composition of acidic NSO compounds in crude oils determined by negative-ion electrospray Fourier transform ion cyclotron resonance mass spectrometry. Organic Geochemistry 78, 23–31.

Liu, Y., Wan, Y.Y., Zhu, Y.J., Fei, C.S., Shen, Z.D., Ying, Y.X., 2020. Impact of biodegradation on polar compounds in crude oil: comparative simulation of biodegradation from two aerobic bacteria using ultrahigh-resolution mass spectrometry. Energy & Fuels 34, 5553–5565.

Liu, Z., Wang, H., Blackbourn, G., Ma, F., He, Z., Wen, Z., Wang, Z., Yang, Z., Luan, T., Wu, Z., 2019. Heavy oils and oil sands: global distribution and resource assessment. Acta Geologica Sinica - English Edition 93, 199–212.

Mackenzie, A., Wolff, G., Maxwell, J., 1983. Fatty acids in some biodegraded petroleums. Possible origins and significance. In: Bjorøy et al. (Eds.) Advances in Organic Geochemistry 1983, John Wiley, Chichester, 637-649.

Martins, L.L., Pudenzi, M.A., da Cruz, G.F., Nascimento, H.D.L., Eberlin, M.N., 2017. Assessing biodegradation of Brazilian crude oils via characteristic profiles of O_1 and O_2 compound classes: petroleomics by negative ion mode electrospray ionization Fourier transform ion cyclotron resonance mass spectrometry. Energy & Fuels 31, 6649–6657.

Meredith, W., Kelland, S.J., Jones, D.M., 2000. Influence of biodegradation on crude oil acidity and carboxylic acid composition. Organic Geochemistry 31, 1059–1073.

Oldenburg, T.B.P., Brown, M., Bennett, B., Larter, S.R., 2014. The impact of thermal maturity level on the composition of crude oils, assessed using ultra-high resolution mass spectrometry. Organic Geochemistry 75, 151–168.

Oldenburg, T.B.P., Jones, M., Huang, H., Bennett, B., Shafiee, N.S., Head, I., Larter, S.R., 2017. The controls on the composition of biodegraded oils in the deep subsurface – Part 4. Destruction and production of high molecular weight non-hydrocarbon species and destruction of aromatic hydrocarbons during progressive in-reservoir biodegradation. Organic Geochemistry 114, 57–80.

Pan, Y.H., Liao, Y.H., Shi, Q., Hsu, C.S., 2013. Acidic and neutral polar NSO compounds in heavily biodegraded oils characterized by negative-ion ESI FT-ICR MS. Energy & Fuels 27, 2960–2973.

Pan, Y.H., Liao, Y.H., Shi, Q., 2017. Variations of acidic compounds in crude oil during simulated aerobic biodegradation: monitored by semiquantitative negative-Ion ESI FT-ICR MS. Energy & Fuels 31, 1126–1135.

Peters, K.E., Walters, C.C., Moldowan, J., 2005. The Biomarker Guide, 2nd Ed.,. Cambridge University Press.

Poetz, S., Horsfield, B., Wilkes, H., 2014. Maturity-driven generation and transformation of acidic compounds in the organic-rich Posidonia shale as revealed by electrospray ionization Fourier transform ion cyclotron resonance mass spectrometry. Energy & Fuels 28, 4877–4888.

Qi, J.F., Li, X.G., Yu, F.S., Yu, T.C., 2013. Cenozoic structural deformation and expression of the "Tan-Lu Fault Zone" in the West Sag of the Liaohe Depression, Bohaiwan basin province, China. Science China: Earth Sciences 43, 1324–1337 (in Chinese with English abstract).

Qian, K., Robbins, W.K., Hughey, C.A., Cooper, H.J., Rodgers, R.P., Marshall, A.G., 2001a. Resolution and identification of elemental compositions for more than 3000 crude acids in heavy petroleum by negative-ion microelectrospray high-field Fourier transform ion cyclotron resonance mass spectrometry. Energy & Fuels 15, 1505–1511.

Qian, K., Rodgers, R.P., Hendrickson, C.L., Emmett, M.R., Marshall, A.G., 2001b. Reading chemical fine print: resolution and identification of 3000 nitrogen-containing aromatic compounds from a single electrospray ionization Fourier transform ion cyclotron resonance mass spectrum of heavy petroleum crude oil. Energy & Fuels 15, 492–498.

Rocha, Y.d.S., Pereira, R.C.L., Mendonça Filho, J.G., 2018. Geochemical characterization of lacustrine and marine oils from off-shore Brazilian sedimentary basins using negative-ion electrospray Fourier transform ion cyclotron resonance mass spectrometry (ESI FTICR-MS). Organic Geochemistry 124, 29-45.

Rojas-Ruiz, F.A., Orrego-Ruiz, J.A., 2016. Distribution of oxygen-containing compounds and its significance on total organic acid content in crude oils by esi negative ion FT-ICR MS. Energy & Fuels 30, 8185–8191.

Sakai, L., Pudenzi, M.A., Nascimento, C.A., Schulz, H., da Cruz, G.F., Martins, L.L., 2021. Significance of acidic polar species assessed by FT-ICR MS to reveal geochemical information of oils from the Sergipe-Alagoas Basin. Abstract, 30th International Meeting on Organic Geochemistry. https://doi.org/10.3997/2214-4609.202134179.

Shi, J., Xiang, M., Qu, D., 2001. Simulation experiments for evolution of fatty acids in immature source rocks. Chinese Science Bulletin 46, 2092–2096.

Shi, Q., Hou, D.J., Chung, K.H., Xu, C.M., Zhao, S.Q., Zhang, Y.H., 2010a. Characterization of heteroatom compounds in a crude oil and its saturates, aromatics, resins, and asphaltenes (SARA) and non-basic nitrogen fractions analyzed by negative-ion electrospray ionization Fourier transform ion cyclotron resonance mass spectrometry. Energy & Fuels 24, 2545–2553.

Shi, Q., Zhao, S.Q., Xu, Z.M., Chung, K.H., Zhang, Y.H., Xu, C.M., 2010b. Distribution of acids and neutral nitrogen compounds in a Chinese crude oil and its fractions: Characterized by negative-ion electrospray ionization Fourier transform ion cyclotron resonance mass spectrometry. Energy & Fuels 24, 4005–4011.

Sun, P., Cai, C., Tang, Y., Tao, Z., Zhao, W., 2020. A new approach to investigate effects of biodegradation on pyrrolic compounds by using a modified Manco scale. Fuel 265, 116937.

Tissot, B.P., Welte, D.H., 1984. Petroleum Formation and Occurrence, 2nd ed. Springer-Verlag, Berlin.

Vaz, B.G., Silva, R.C., Klitzke, C.F., Simas, R.C., Nascimento, H.D.L., Pereira, R.C.L., Garcia, D.F., Eberlin, M.N., Azevedo, D.A., 2013. Assessing biodegradation in the Llanos Orientales crude oils by electrospray ionization ultrahigh resolution and accuracy Fourier transform mass spectrometry and chemometric analysis. Energy & Fuels 27, 1277–1284.

Vogel, T.M., Grbìc-Galìc, D., 1986. Incorporation of oxygen from water into toluene and benzene during anaerobic fermentative transformation. Applied and Environmental Microbiology 52, 200–202.

Volkman, J.K., 1986. A review of sterol markers for marine and terrigenous organic matter. Organic Geochemistry 9, 83–99.

Wan, Z.H., Li, S.M., Pang, X.Q., Dong, Y.X., Wang, Z.J., Chen, X.F., Meng, X.B., Shi, Q., 2017. Characteristics and geochemical significance of heteroatom compounds in terrestrial oils by negative-ion electrospray Fourier transform ion cyclotron resonance mass spectrometry. Organic Geochemistry 111, 34–55.

Wang, W., Liu, L., Jiang, Z., Zhong, N., Wang, Y., Wang, P., Wu, L., Meng, J., Zhou, J., Guo, Y., 2011. Geochemistry of source rocks in the Es_3 and Es_4 members in the Shahejie Formation of the Western Depression, Liaohe Oilfield, China. Chinese Journal of Geochemistry 30, 405–414.

Wenger, L.M., Davis, C.L., Isaksen, G.H., 2002. Multiple controls on petroleum biodegradation and impact on oil quality. SPE Reservoir Evaluation & Engineering 5, 375–383.

Xiong, Y., Geng, A., Wang, C., Sheng, G., Fu, J., 2003. The origin of crude oils from the Shuguang-Huanxiling Buried Hills in the Liaohe Basin, China: Evidence from chemical and isotopic compositions. Applied Geochemistry 18, 445–456.

Zhan, D., Fenn, J.B., 2000. Electrospray mass spectrometry of fossil fuels. International Journal of Mass Spectrometry 194, 197–208.

Zhang, Y., Liao, Y., Guo, S., Xu, C., Shi, Q., 2016. Molecular transformation of crude oil in confined pyrolysis system and its impact on migration and maturity geochemical parameters. Energy & Fuels 30, 6923–6932.

Ziegs, V., Noah, M., Poetz, S., Horsfield, B., Hartwig, A., Rinna, J., Skeie, J.E., 2018. Unravelling maturity- and migration-related carbazole and phenol distributions in Central Graben crude oils. Marine and Petroleum Geology 94, 114–130.